

## Supplemental information

### Supplementary figures:

**Supplementary figure 1.** Cre-recombinase and RAR $\alpha$  expression in intestinal epithelial cells from the RAR $\alpha^{\text{villin}}$  mice. **(a-b)** Frozen sections from the proximal, medial and distal small intestine and colon were stained for Cre-recombinase **(a)** and RAR $\alpha$  **(b)**. One representative figure out of three.

TA, transit amplifying

**Supplementary figure 2.** Stem cell compartment is not significantly altered after RAR $\alpha$  inhibition. **(a)** OLFM4 expression was detected by immunostaining on frozen sections of small intestine from both wild type and RAR $\alpha$  villin mice. **(b)** Position and **(c)** Number of positive OLF4 cells per crypt were counted in 10 -12 crypts across 3 different sections of small intestine in two different mice per genotype. \*P < 0.05; \*\*P < 0.01; \*\*\* P < 0.005; Student's t-test. Results are shown as mean  $\pm$  SEM. Scale bar 100uM.

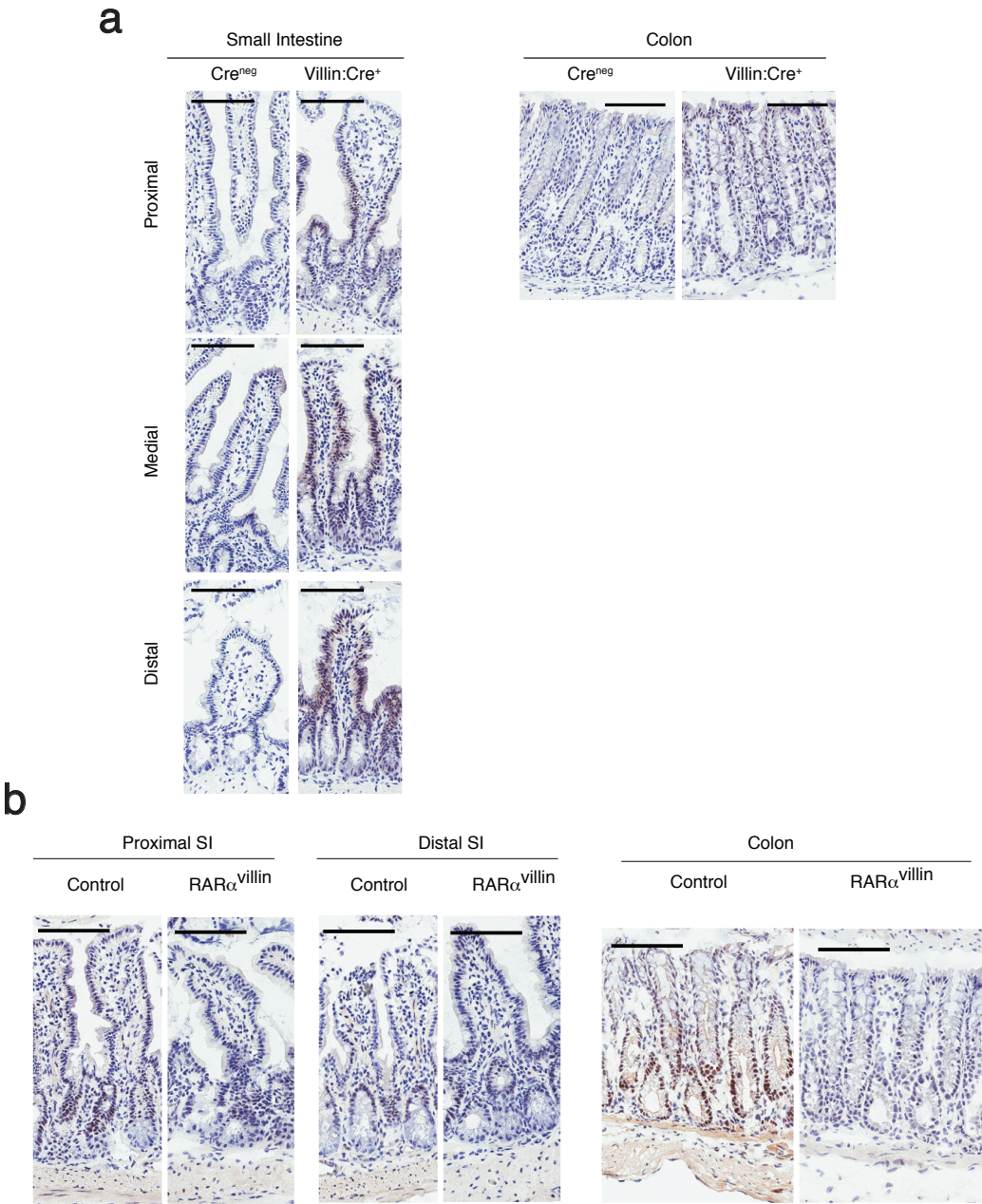
**Supplementary figure 3.** Altered proliferating cell distribution in mice lacking RAR $\alpha$  specifically in intestinal epithelial cells. Cleaved caspase 3 **(a)** and Ki-67 levels in the small intestine (SI, panels **b**, **c**) and colon (panels **d** and **e**) was determined by immunohistochemistry. The number of Caspase 3<sup>+</sup> and Ki-67<sup>+</sup> cells relative to their position along the crypt-villus axis was counted in at least 5 different crypts in 2 fields of view per sample (10x). **(f)** Crypt length was quantified by cell number/crypt. Data are representative of three mice.

**Supplementary figure 4.** Defining myeloid cell population in tSNE plots. Cell suspensions from small intestinal lamina propria were analyzed by FACS and datasets were exported, concatenated

and displayed in t-distributed stochastic linear embedding (tSNE) analysis (one representative analysis of two). Heat maps show the level of expression of CD11c, F4/80, CD11b and CD103.

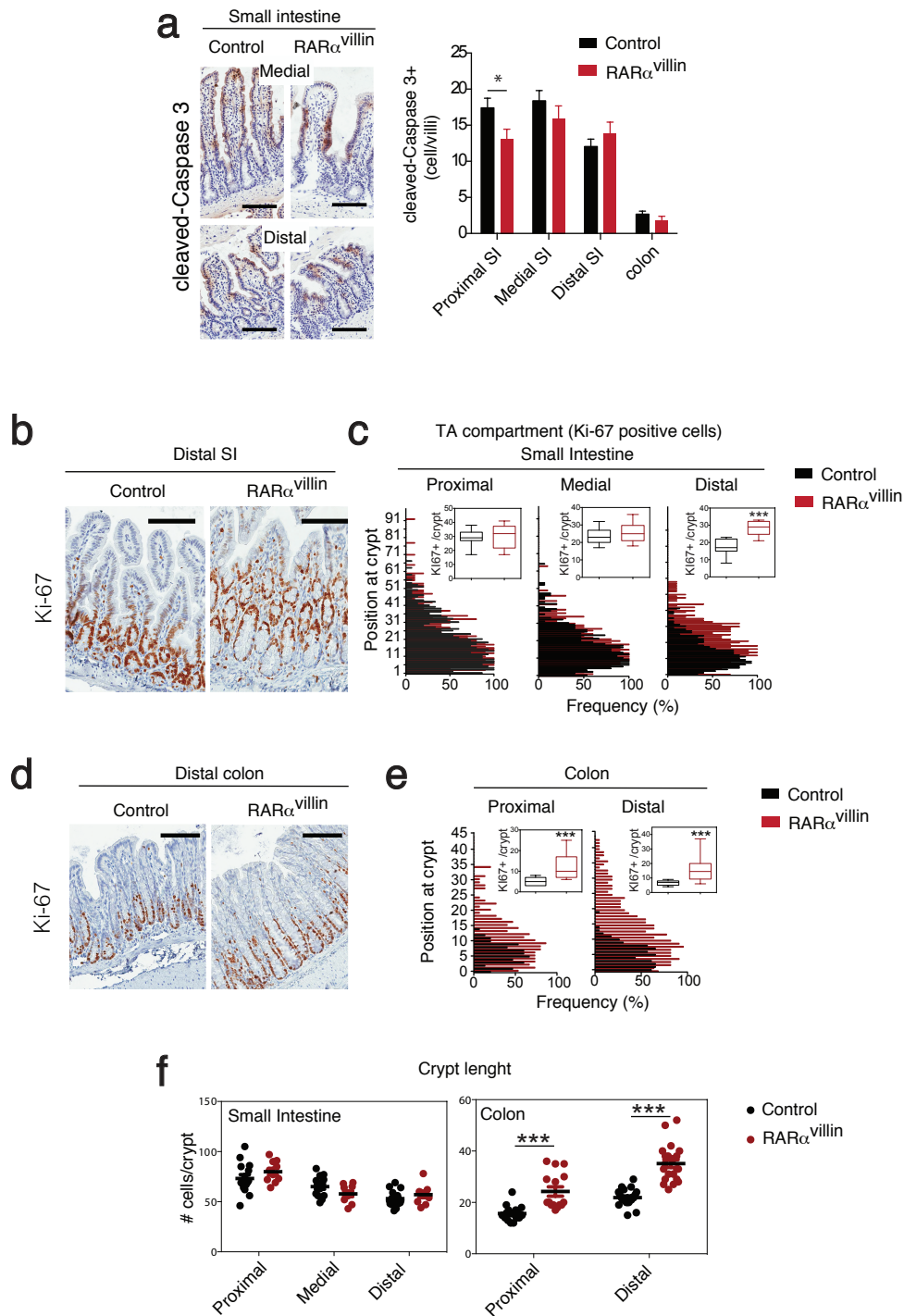
**Supplementary figure 5.** Identification of cryptopatches by immunohistochemistry Expression of CD3, CD11c, and CD90 in the small intestine was determined by immunohistochemistry. Cell clusters expressing CD90 (**a**) were further analyzed for expression of CD11c and CD3 (**b**). Cell clusters expressing CD90 and CD11c but negative for CD3 were considered to be bona fide cryptopatches. PP; Peyer's Patches. (**c**) Cryptopatches analysis was performed in swiss rolls from the small intestine and colon from control and  $RAR\alpha^{villin}$  mice. One representative figure out of three.

# Supplementary figure 1



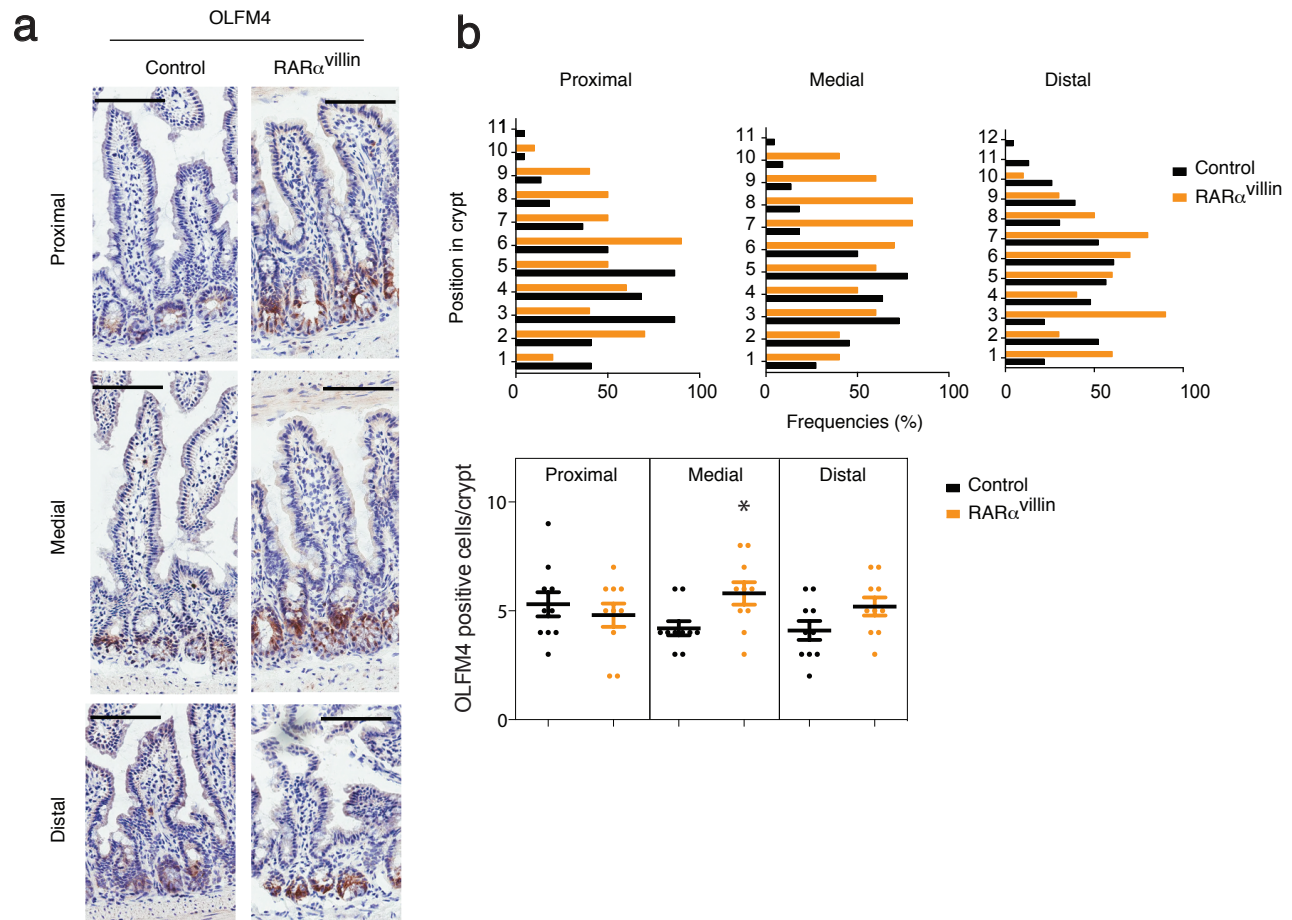
Supplementary figure 1. Cre-recombinase and RAR $\alpha$  expression in intestinal epithelial cells from the RAR $\alpha$ <sup>villin</sup> mice. (a-b) Frozen sections from the proximal, medial and distal small intestine and colon were stained for Cre-recombinase (a) and RAR $\alpha$  (b). One representative figure out of three. TA, transit amplifying. Scale bar 100uM.

## Supplementary figure 2



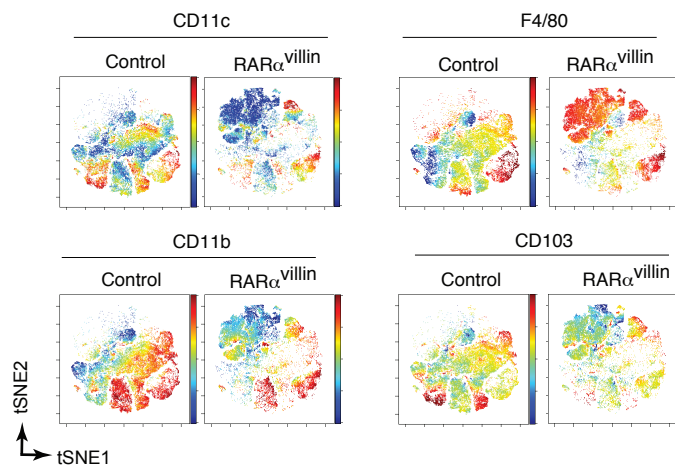
Supplementary figure 2. Altered proliferating cell distribution in mice lacking RAR $\alpha$  specifically in intestinal epithelial cells. Cleaved caspase 3 (a) and Ki-67 levels in the small intestine (SI, panels b, c) and colon (panels d and e) was determined by immunohistochemistry. The number of Caspase 3<sup>+</sup> and Ki-67<sup>+</sup> cells relative to their position along the crypt-villus axis was counted in at least 5 different crypts in 2 fields of view per sample (10x). (f) Crypt length was quantified by cell number/crypt. Data are representative of three mice. Scale bar 100uM

## Supplementary figure 3



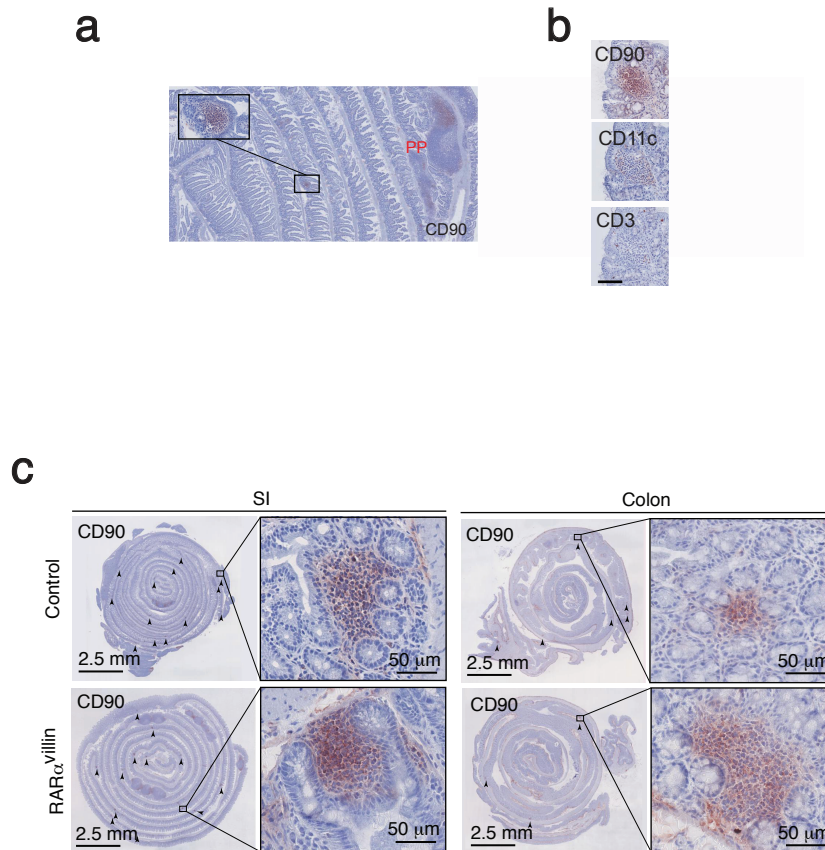
Supplementary figure 3. Stem cell compartment is not significantly altered after RAR $\alpha$  inhibition. (a) OLFM4 expression was detected by immunostaining on frozen sections of small intestine from both wild type and RAR $\alpha$ <sup>villin</sup> mice. (b) Position and (c) Number of positive OLF4 cells per crypt were counted in 10 -12 crypts across 3 different sections of small intestine in two different mice per genotype. \*P < 0.05; \*\*P < 0.01; \*\*\* P < 0.005; Student's t-test. Results are shown as mean  $\pm$  SEM. Scale bar 100 $\mu$ M.

## Supplementary figure 4



Supplementary figure 4. Defining myeloid cell population in tSNE plots. Cell suspensions from small intestinal lamina propria were analyzed by FACS and datasets were exported, concatenated and displayed in t-distributed stochastic linear embedding (tSNE) analysis (one representative analysis of two). Heat maps show the level of expression of CD11c, F4/80, CD11b and CD103.

## Supplementary figure 5



Supplementary figure 5. Identification of cryptopatches by immunohistochemistry Expression of CD3, CD11c, and CD90 in the small intestine was determined by immunohistochemistry. Cell clusters expressing CD90 (a) were further analyzed for expression of CD11c and CD3 (b). Cell clusters expressing CD90 and CD11c but negative for CD3 were considered to be bona fide cryptopatches. PP; Peyer's Patches. (c) Cryptopatches analysis was performed in swiss rolls from the small intestine and colon from control and RAR $\alpha$ villin mice. One representative figure out of three.